Correlation of Mathematical Model with AFRL RC-19 Aerothermoelastic Experiment Including an Impinging Shock

AIAA AVIATION Forum 2025

Luisa Piccolo Serafim and Earl Dowell – Duke University

Kirk Brouwer – AFRL, Wright-Patterson AFB

July 22, 2025 | Las Vegas, NV

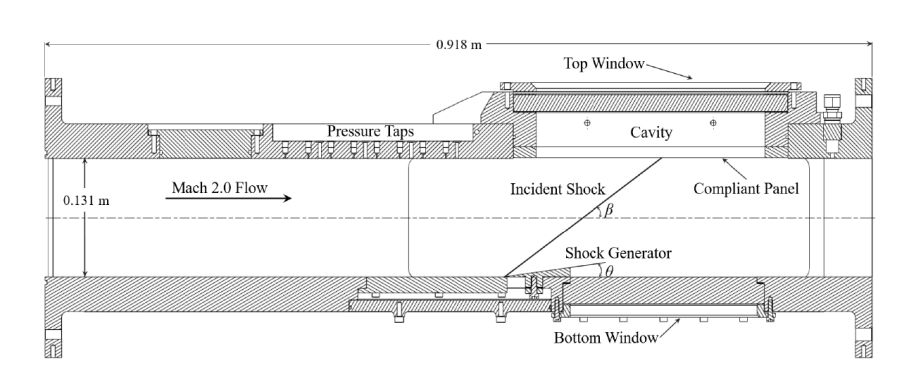


Motivation for this Work

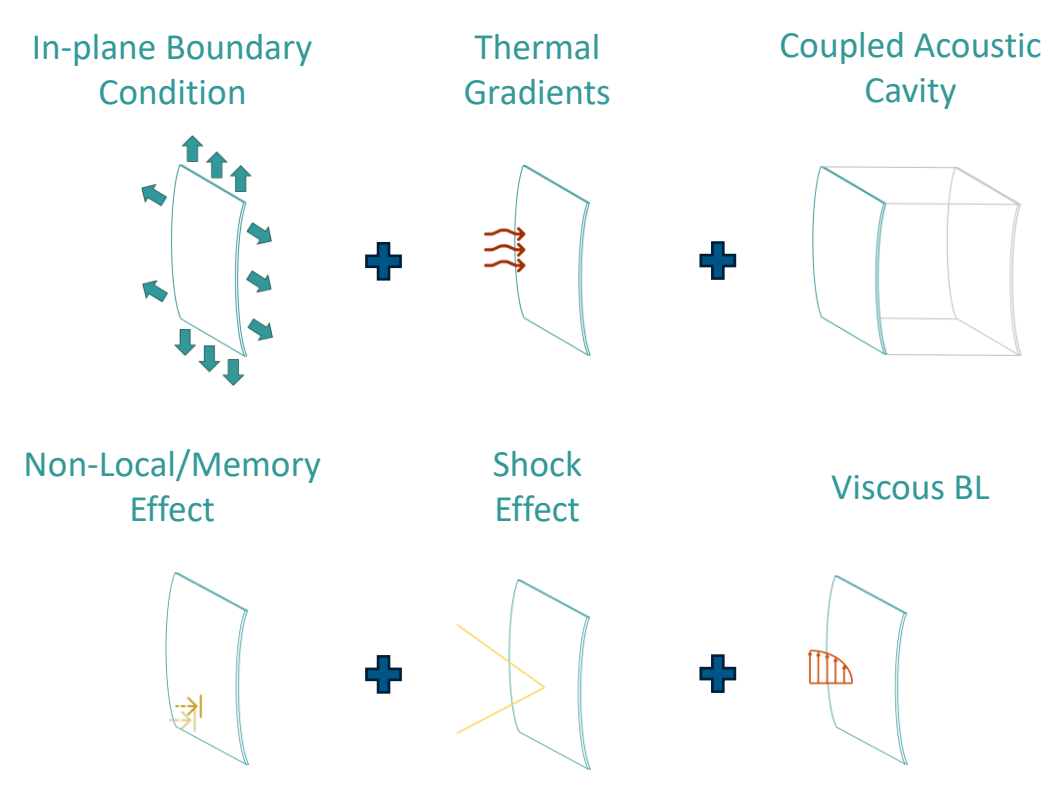
- To provide the highest possible fidelity in the computational model at an affordable cost; orders of magnitude reduction in cost compared to traditional CFD/CSD methods
- To explore a wide range of relevant parameters including M_{∞} , Re, static pressure differential, thermal stresses and structural boundary conditions, both out of plane and in plane.

• To correlate computational results with experimental results and assess the sensitivity of these results to uncertainties

in key parameters



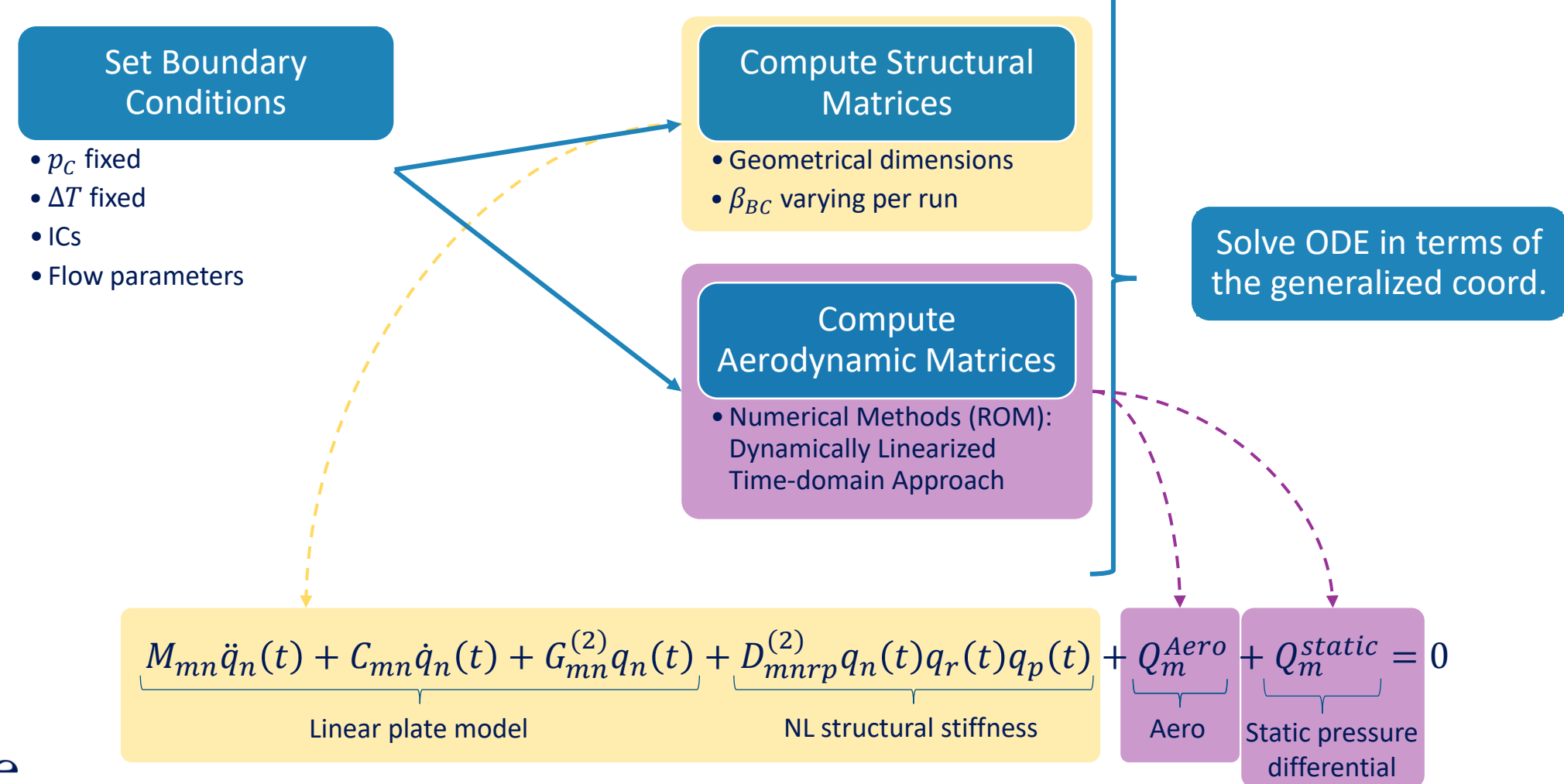






Mathematical/Computational Modeling

Nonlinear Aeroelastic Solver

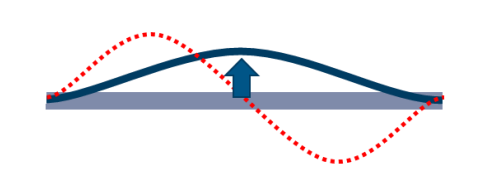




ROM to include unsteady aerodynamics into the aeroelastic solution

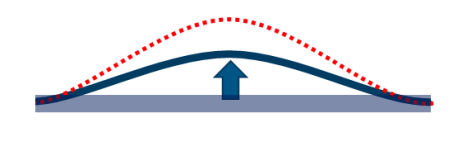
Step change in the CFD domain for each ψ_{mn} ...

... in the panel deformation:



1st set of CFD runs

... in the velocity of the panel deformation:



2nd set of CFD runs

... to obtain a pressure field (output) from a known deformation (input)

$$Q_{mn}^{CFD}(t) = \iint \frac{\Delta p_m(x, y, t)}{\rho_\infty U_\infty^2} \psi_n(x, y) dx dy$$

Work the other way around to obtain the A_{mn} , B_{mn} , and $E_{mn}(t)$ using the input/output relationship

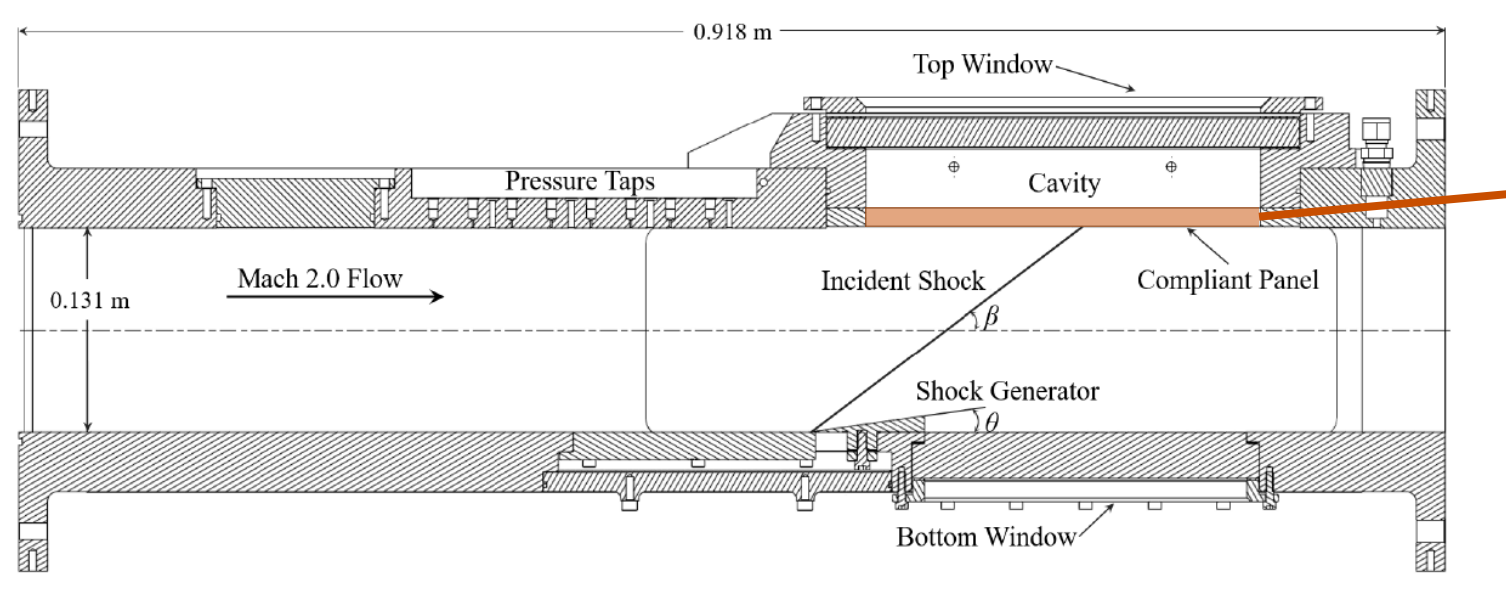
$$Q_{mn}^{CFD}(t) = q_m(t)A_{mn} + \dot{q}_m(t)B_{mn} + \int_0^t q_m(\tau)E_{mn}(t-\tau)d\tau$$

Once A_{mn} , B_{mn} , and $E_{mn}(t)$ are obtained, we can reconstruct the Generalized Aerodynamic Force inside the Aeroelastic Solver for any arbitrary panel deformation $(q_m(t), \dot{q}_m(t))$

$$Q_{mn}(t) = q_m(t)A_{mn} + \dot{q}_m(t)B_{mn} + \int_0^t q_m(\tau)E_{mn}(t-\tau)d\tau$$

Experimental Study Case: AFRL/SD RC-19 Wind Tunnel Section

Additional Considerations: In-plane boundary condition

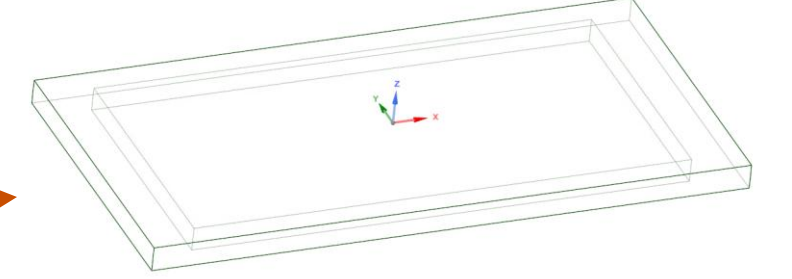


Brouwer et al. AIAAJ (2021)

In-plane boundary stiffness

Nondimensional in-plane boundary stiffness

 $eta_{BC} \equiv \frac{K_{BC}a}{E\hbar}$ Panel length Panel thickness



Nonlinear structural behavior

In-plane boundary stiffness

"allowing the panel to deform at the edges as a reaction to the fixed support"

 $\beta_{BC} \approx 0$: Free edge displacement $\beta_{BC} \gg 0$: No edge displacement

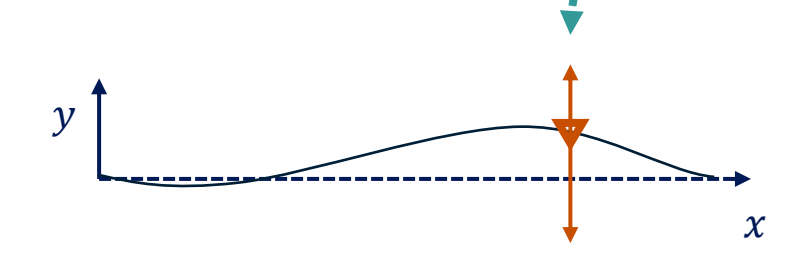
Experimental Study Case: AFRL/SD RC-19 Wind Tunnel Section

Additional Considerations: In-plane boundary condition

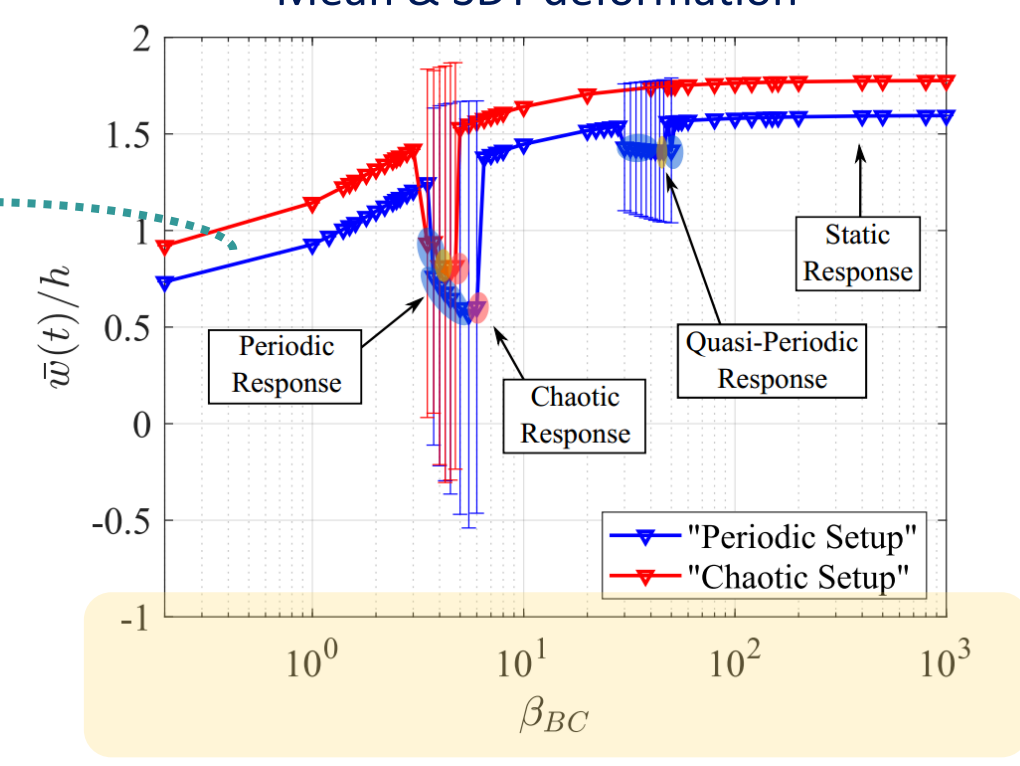
Results are presented as a function of the β_{BC} , which is a **structural** parameter

For example:

Mean and STD of the panel deformation at ¾ of the panel length using Linear Piston Theory as the aerodynamic model



Mean & SDT deformation



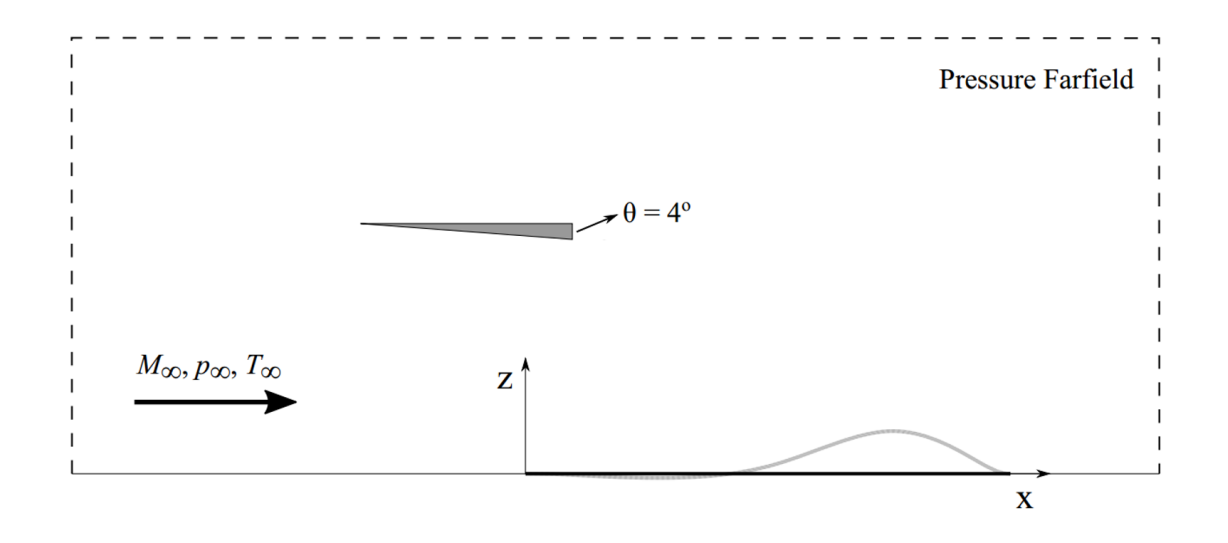


DLTA with a Shock Impingement

 $\theta=4^{\circ}$ wedge shock configuration

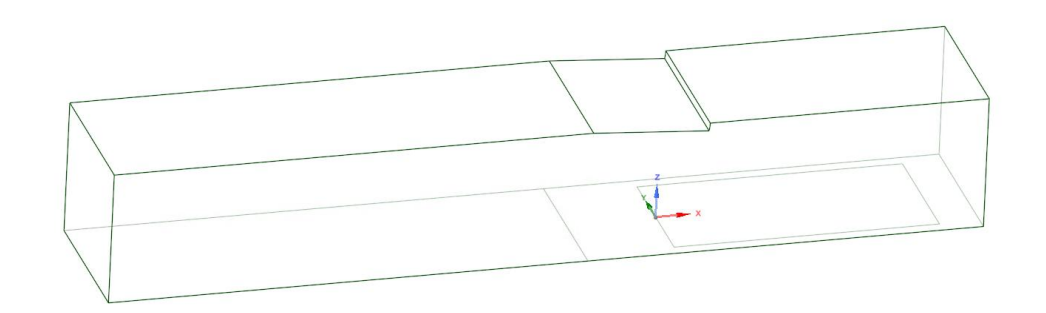
Aerodynamic Model: Euler (unsteady)/DLTA

(Dynamically Linearized Time-Domain Approach)



Aerodynamic Model: RANS (unsteady)/DLTA

(Dynamically Linearized Time-Domain Approach)



In-Plane boundary stiffness sensitivity

$$M_{\infty}=2.0$$

 ΔT between panel and frame Δp between fluid and acoustic cavity

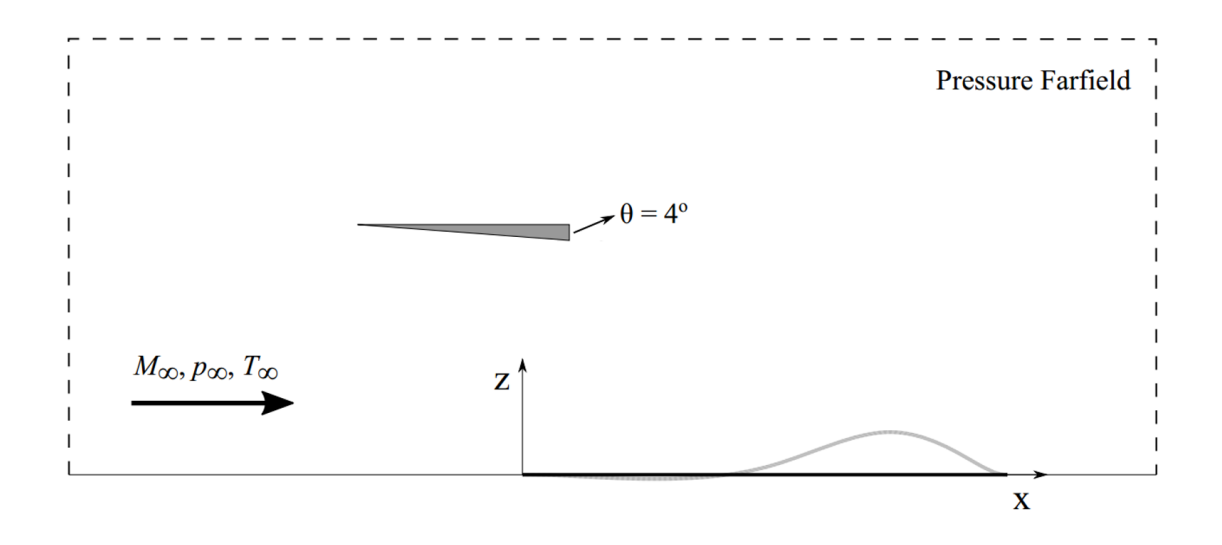


DLTA with a Shock Impingement

 $\theta=4^{\circ}$ wedge shock configuration

Aerodynamic Model: Euler (unsteady)/DLTA

(Dynamically Linearized Time-Domain Approach)



Aerodynamic Model: RANS (unsteady)/DLTA

(Dynamically Linearized Time-Domain Approach)



In-Plane boundary stiffness sensitivity

$$M_{\infty}=2.0$$

 ΔT between panel and frame Δp between fluid and acoustic cavity



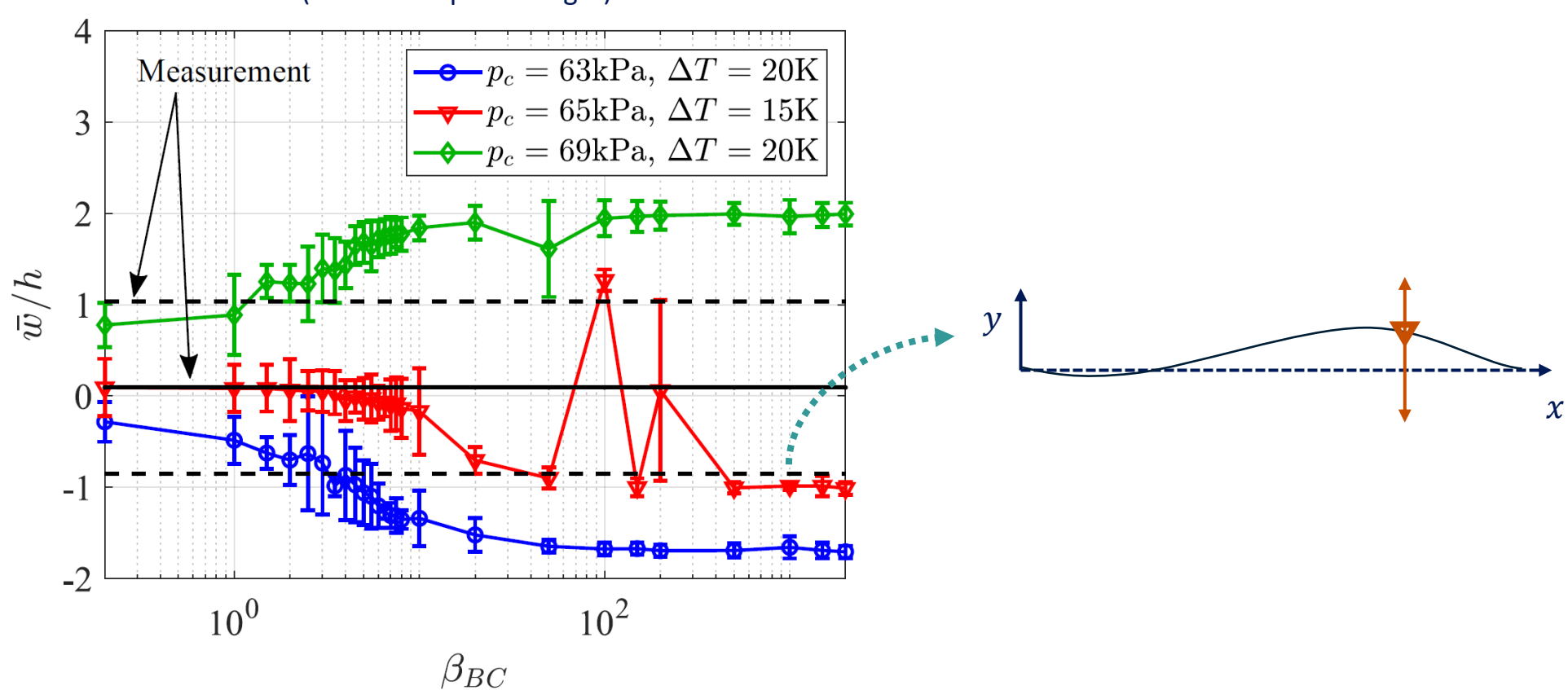
 $\theta=4^{\circ}$ wedge shock configuration

Wind Tunnel Setting

p_c (kPa)	ΔT (K)
68.9	13.3

Mean & SDT deformation

(at ¾ of the panel length)





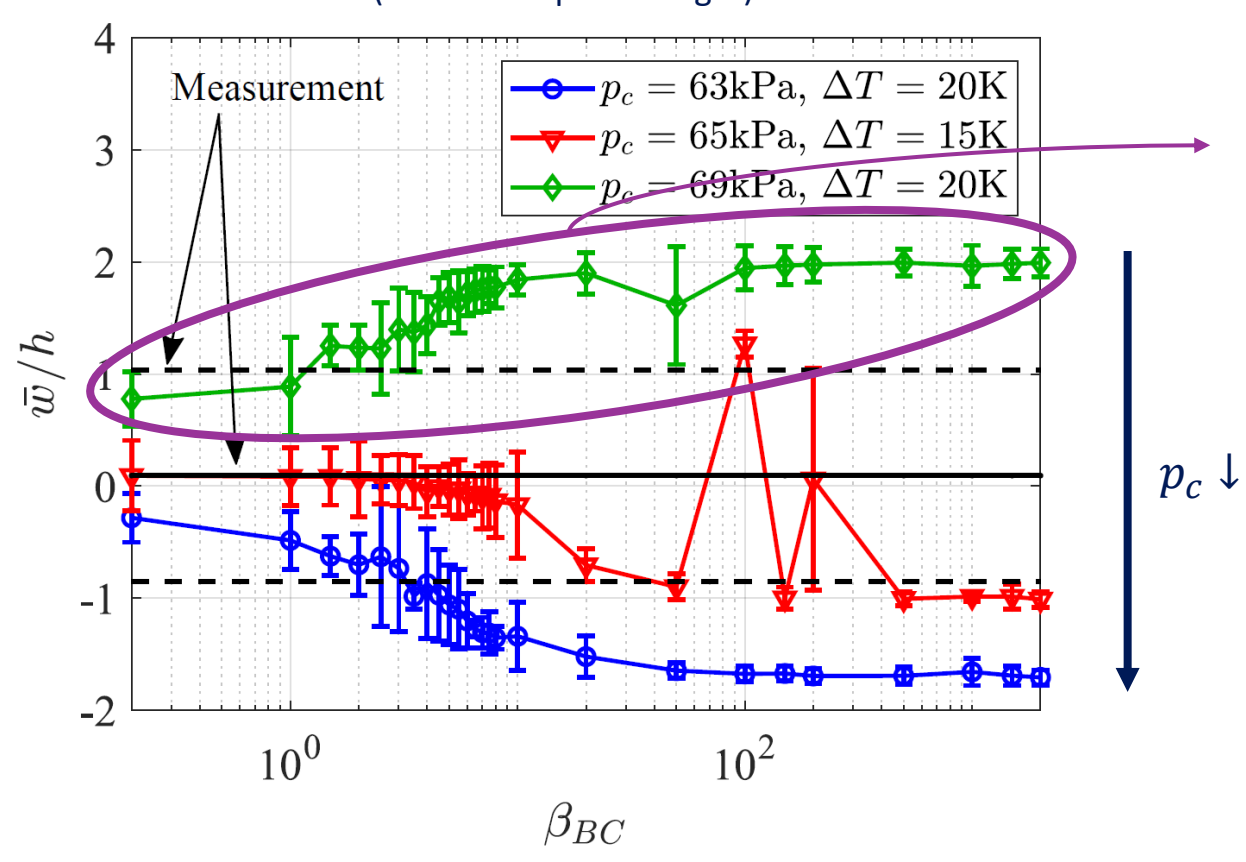
 $\theta=4^{\circ}$ wedge shock configuration

Wind Tunn	el Setting
-----------	------------

p_c (kPa)	ΔT (K)
68.9	13.3

Mean & SDT deformation

(at ¾ of the panel length)



Similar to the wind tunnel setting



 $\theta=4^{\circ}$ wedge shock configuration

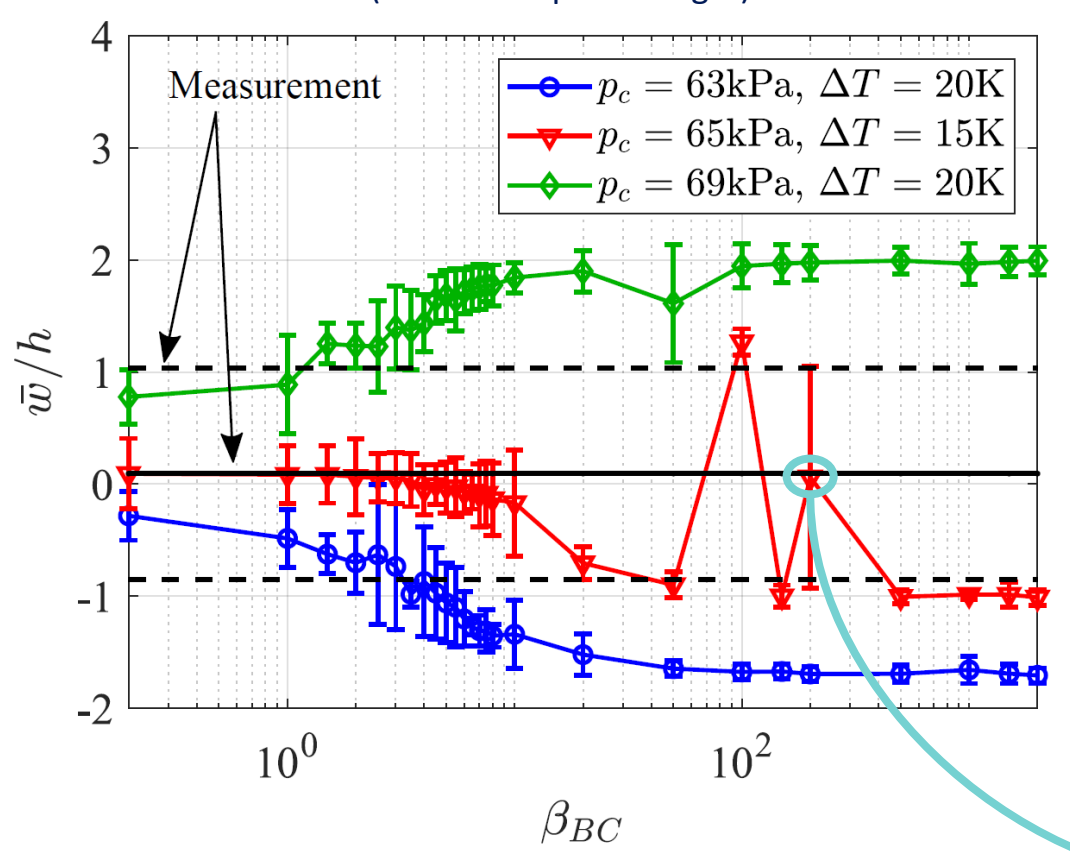
Wind Tunnel Setting

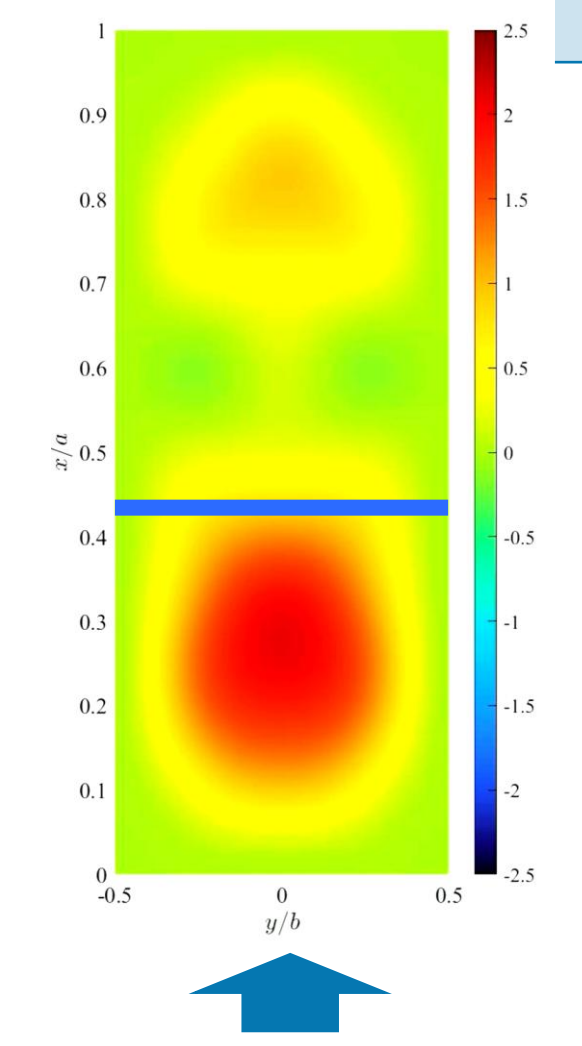
 p_c (kPa) ΔT (K)

68.9

13.3

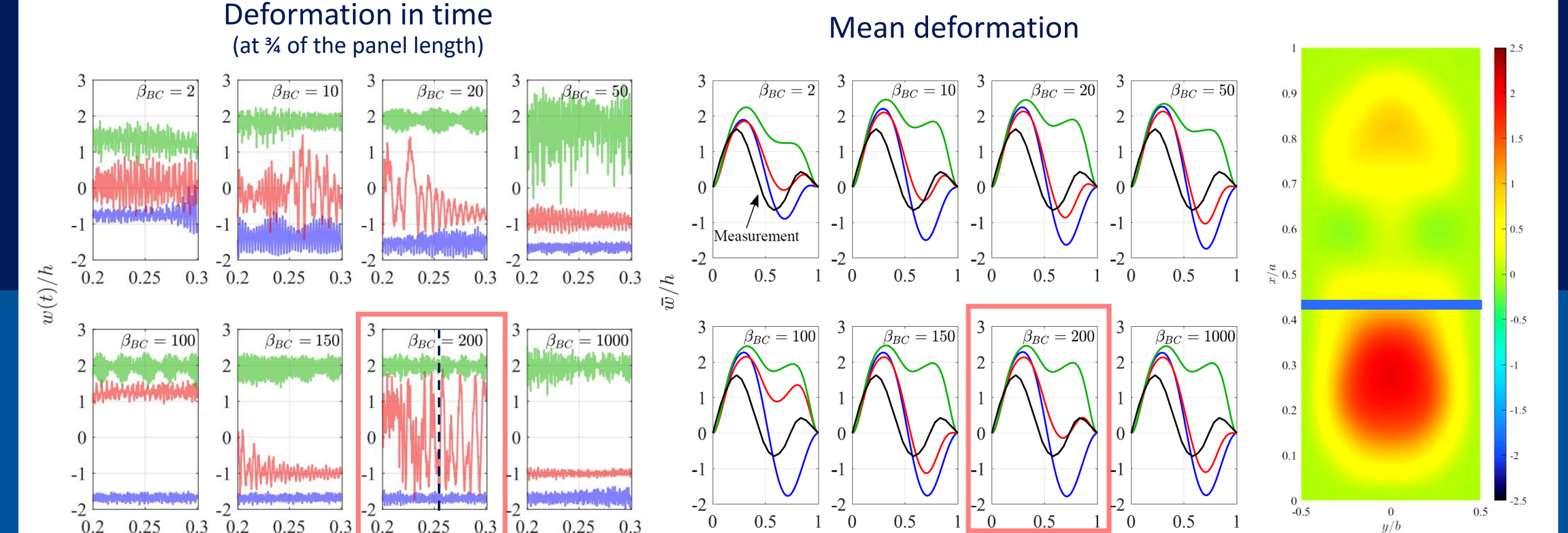
Mean & SDT deformation (at ¾ of the panel length)







Flow Field





Flow Field

 $p_c = 63$ kPa, $\Delta T = 20$ K $p_c = 65$ kPa, $\Delta T = 15$ K

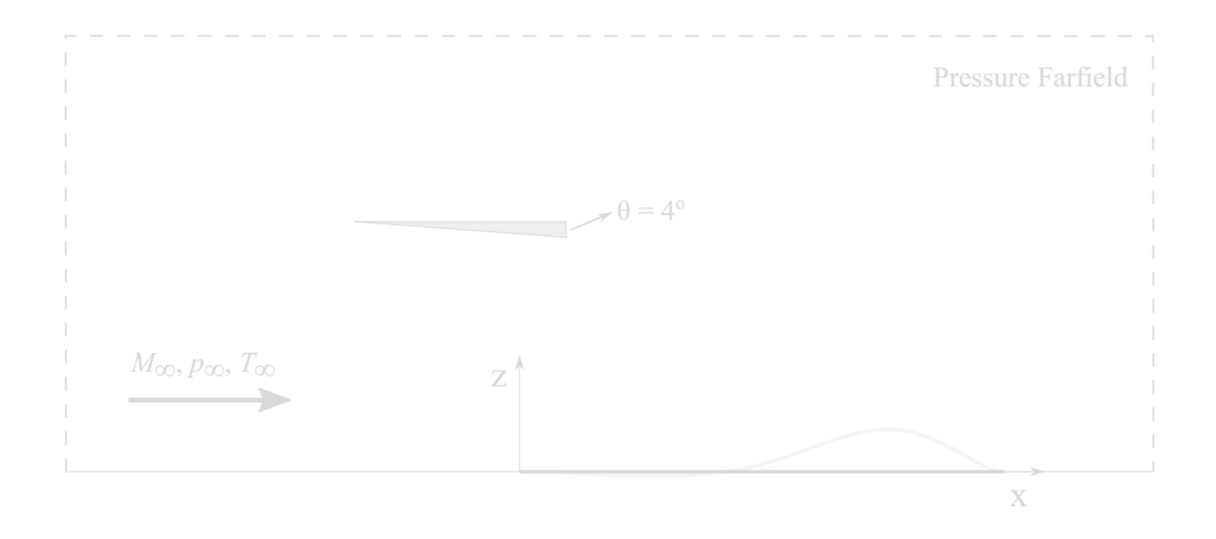
 $- p_c = 69 \text{kPa}, \Delta T = 20 \text{K}$

DLTA with a Shock Impingement

 $\theta = 4^{\circ}$ wedge shock configuration

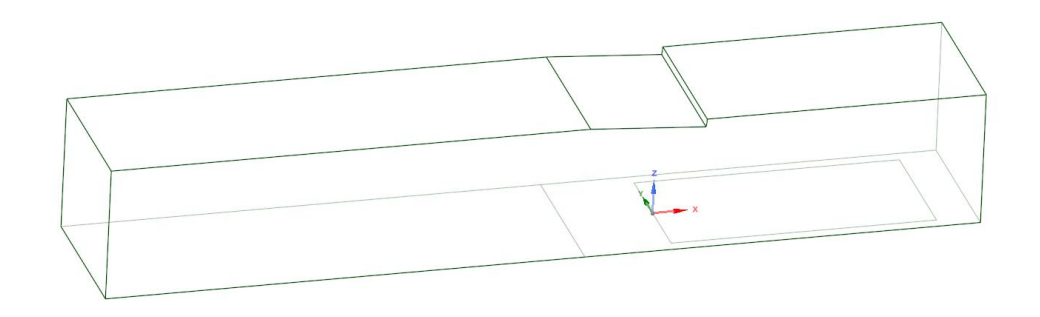
Aerodynamic Model: Euler (unsteady)/DLTA

(Dynamically Linearized Time-Domain Approach)



Aerodynamic Model: RANS (unsteady)/DLTA

(Dynamically Linearized Time-Domain Approach)



In-Plane boundary stiffness sensitivity

$$M_{\infty}=2.0$$

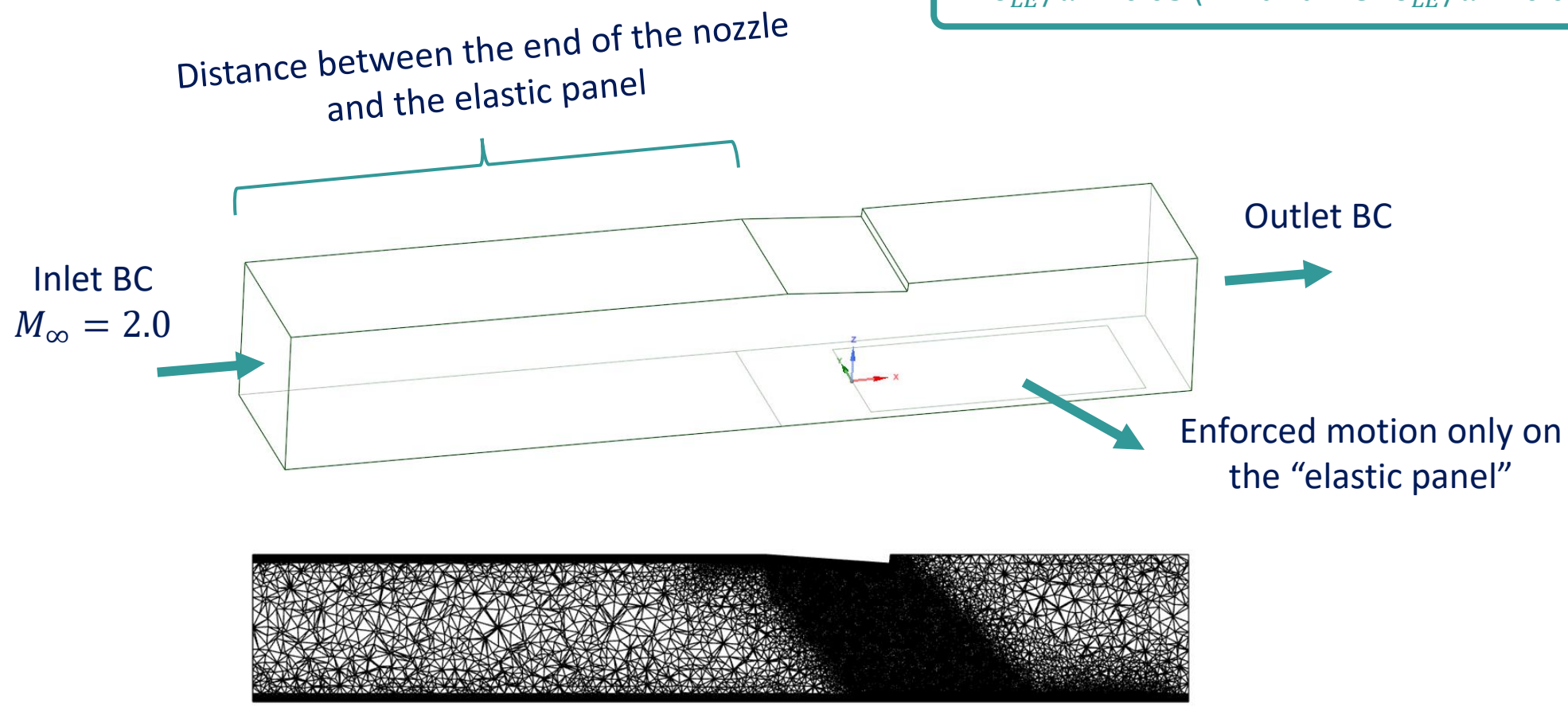
 ΔT between panel and frame Δp between fluid and acoustic cavity



DLTA with a Shock Impingement

 $\theta=4^{\circ}$ wedge shock configuration: CFD setup

 $\begin{array}{c} \operatorname{SST} k - \omega \\ y^+ = 5 \text{ and } 1 \\ \delta_{LE} \approx \operatorname{8mm} \text{ (Wind Tunnel: } \delta_{LE} \approx \operatorname{8.6mm} \text{)} \\ \delta_{LE}/a \approx 0.03 \text{ (Wind Tunnel: } \delta_{LE}/a \approx 0.033 \text{)} \end{array}$





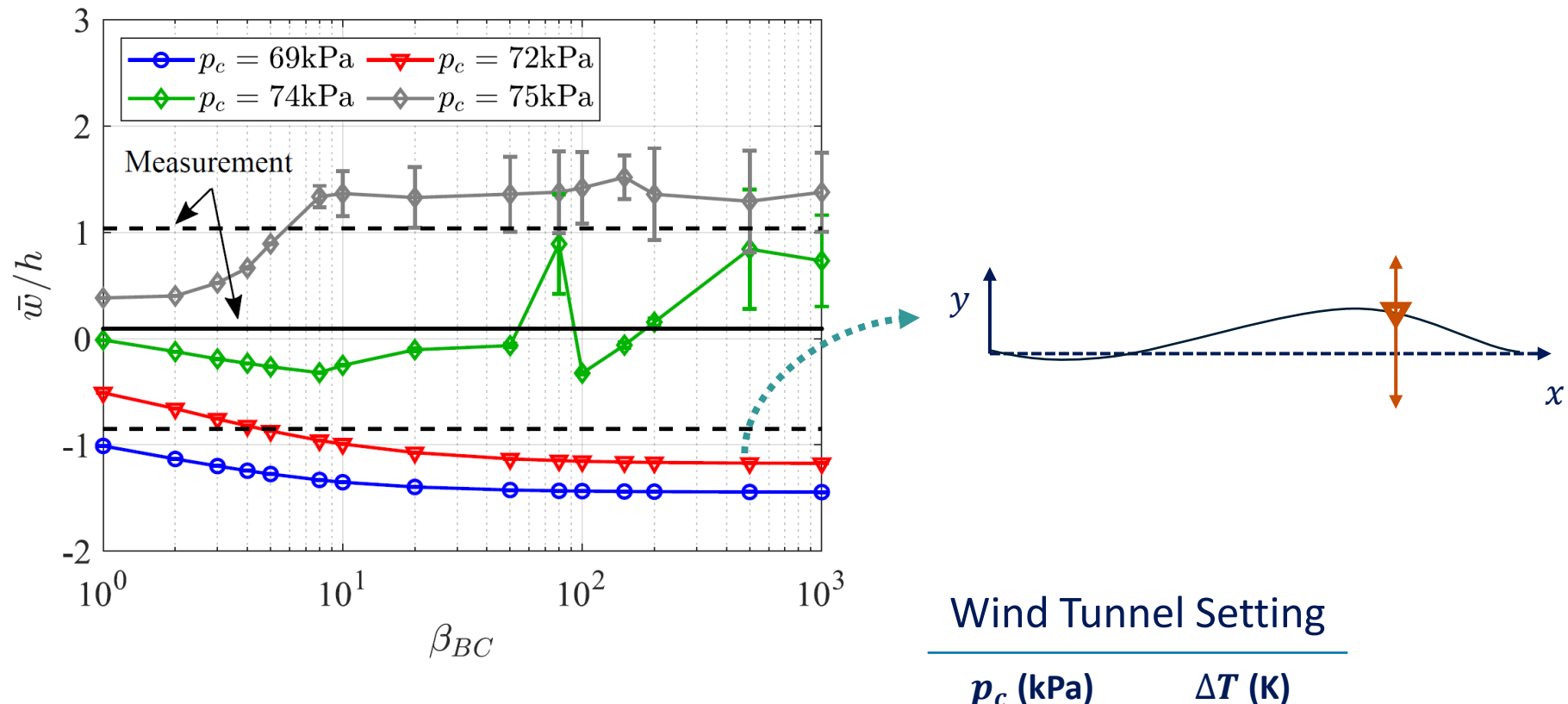
$\Delta T = 15 \text{ K}$ $y^+ = 1$

DLTA with a Viscous Shock Impingement

 $\theta=4^{\circ}$ wedge shock configuration

Mean & SDT deformation

(at ¾ of the panel length)



Duke

p_c (kPa)	ΔT (K)
68.9	13.3

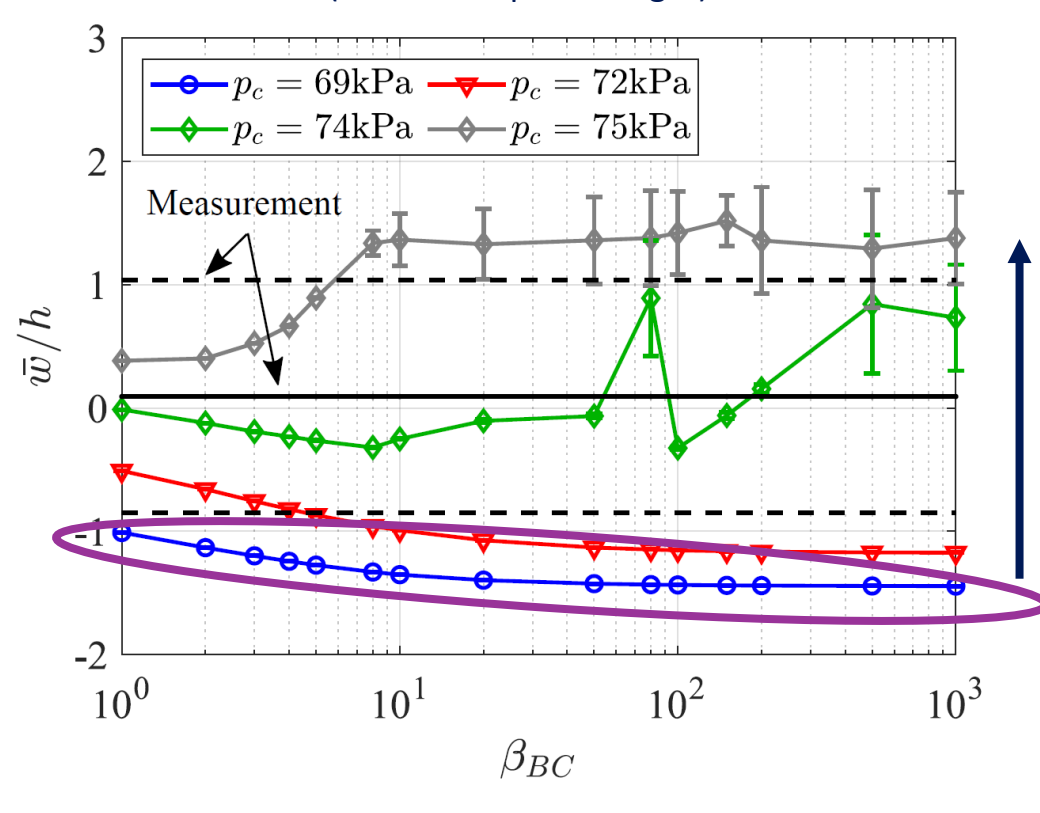
$\Delta T = 15 \text{ K}$ $y^+ = 1$

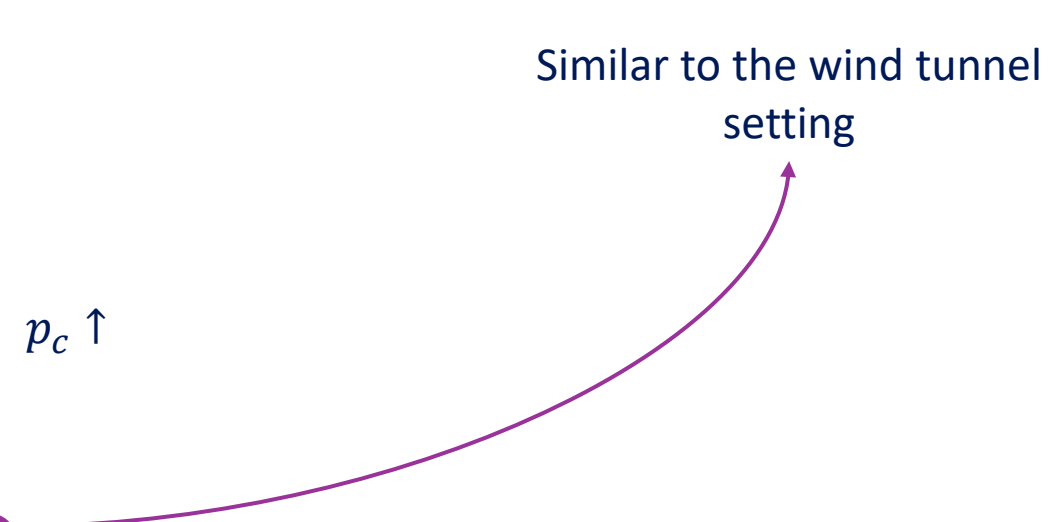
DLTA with a Viscous Shock Impingement

 $\theta=4^{\circ}$ wedge shock configuration

Mean & SDT deformation

(at ¾ of the panel length)





Wind Tunnel Setting

$oldsymbol{p}_c$ (kPa)	ΔT (K)
68.9	13.3

Duke

DLTA with a Viscous Shock Impingement

 $\theta = 4^{\circ}$ wedge shock configuration

Mean & SDT deformation

(at ¾ of the panel length)

 10^2

 β_{BC}

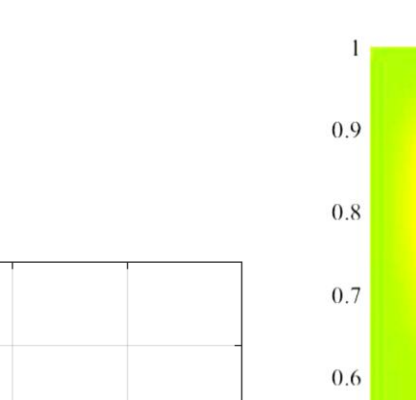
 $- p_c = 69 \text{kPa} - p_c = 72 \text{kPa}$

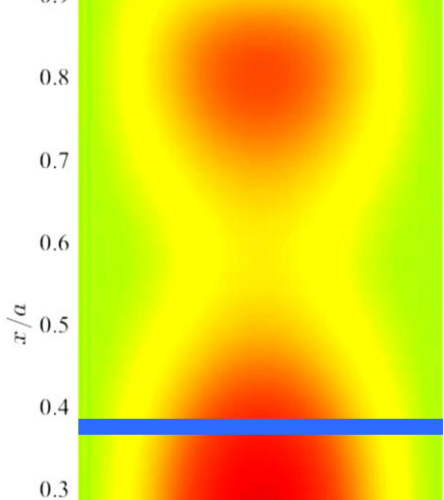
 10^1

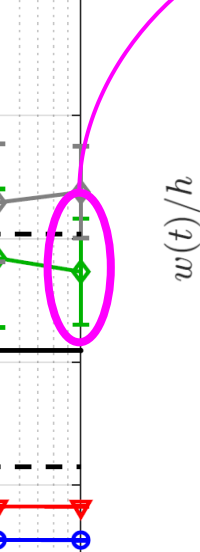
Measurement

$\Delta T = 15 \text{ K}$ $y^{+} = 1$

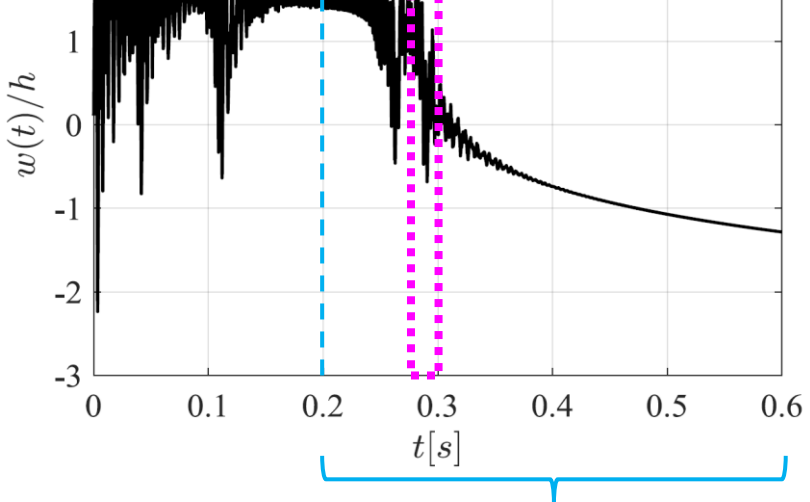
-0.5

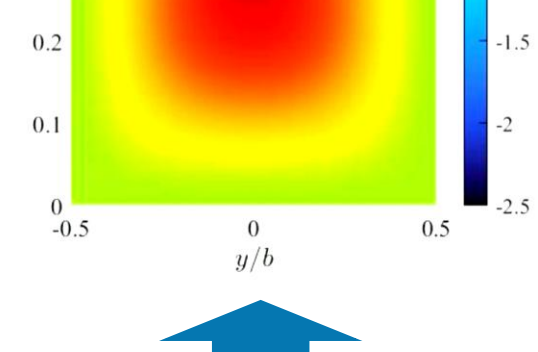






 10^3





Flow Field

Wind Tunnel Setting

$oldsymbol{p}_c$ (kPa)	ΔT (K)
68.9	13.3

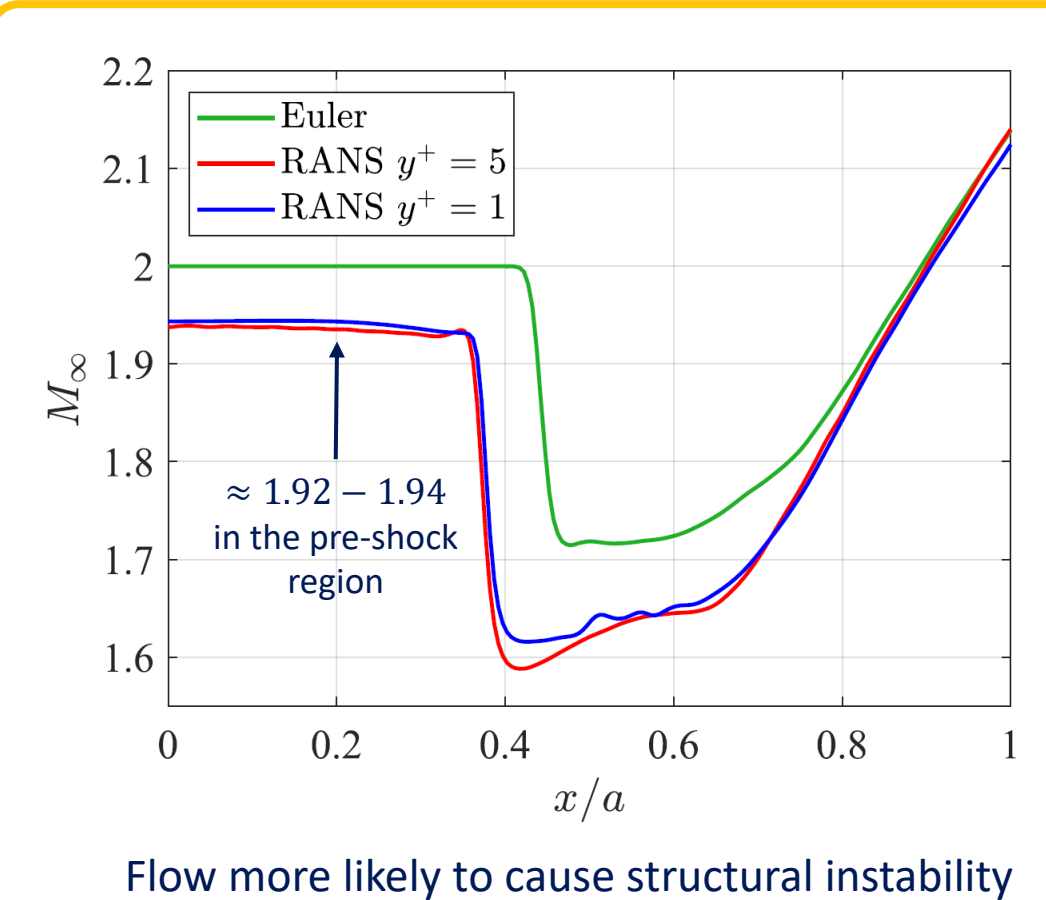
 10^0

 $ar{w}/h$

Shock Impingement Aerodynamic Properties

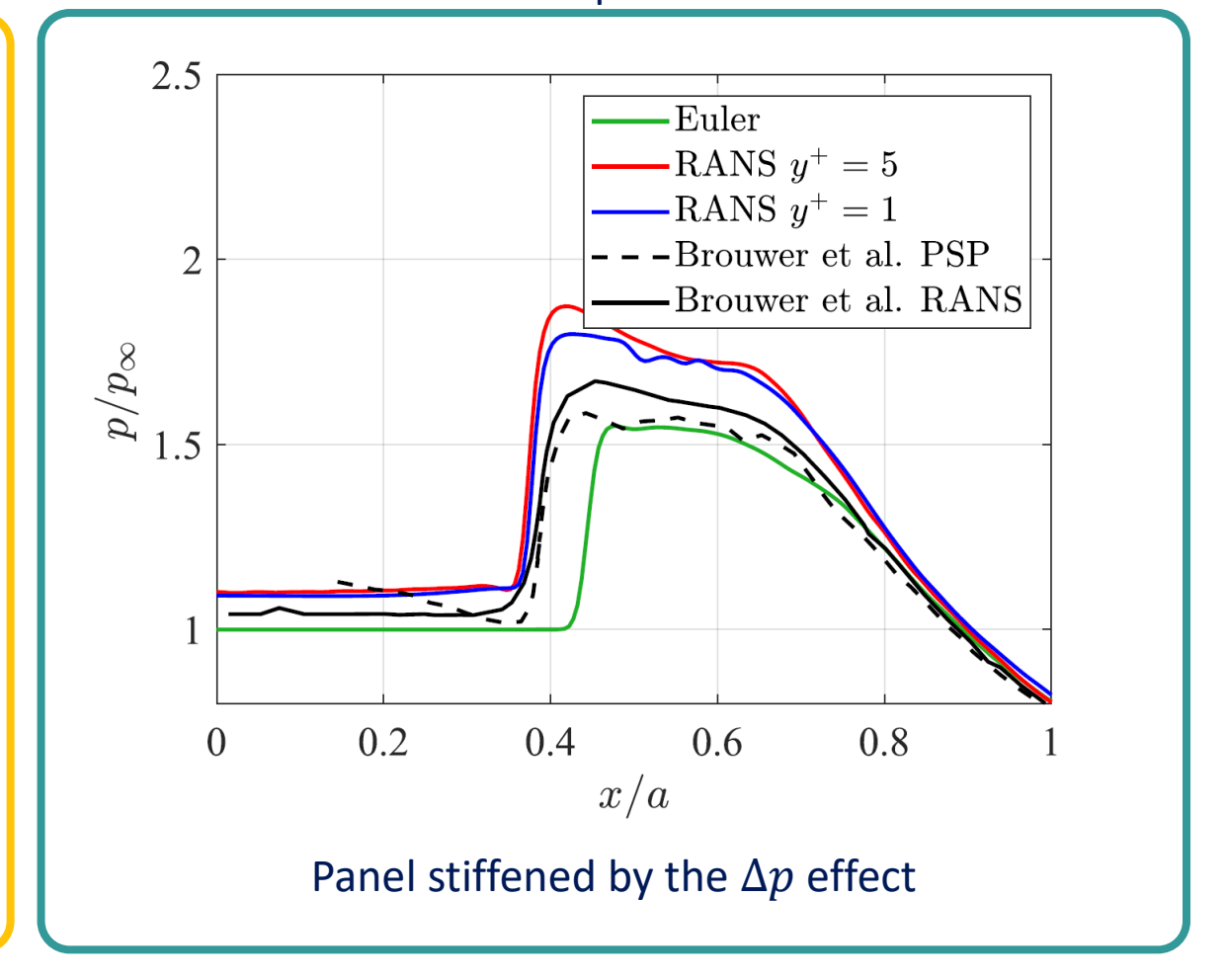
Steady Solution

Local Mach number



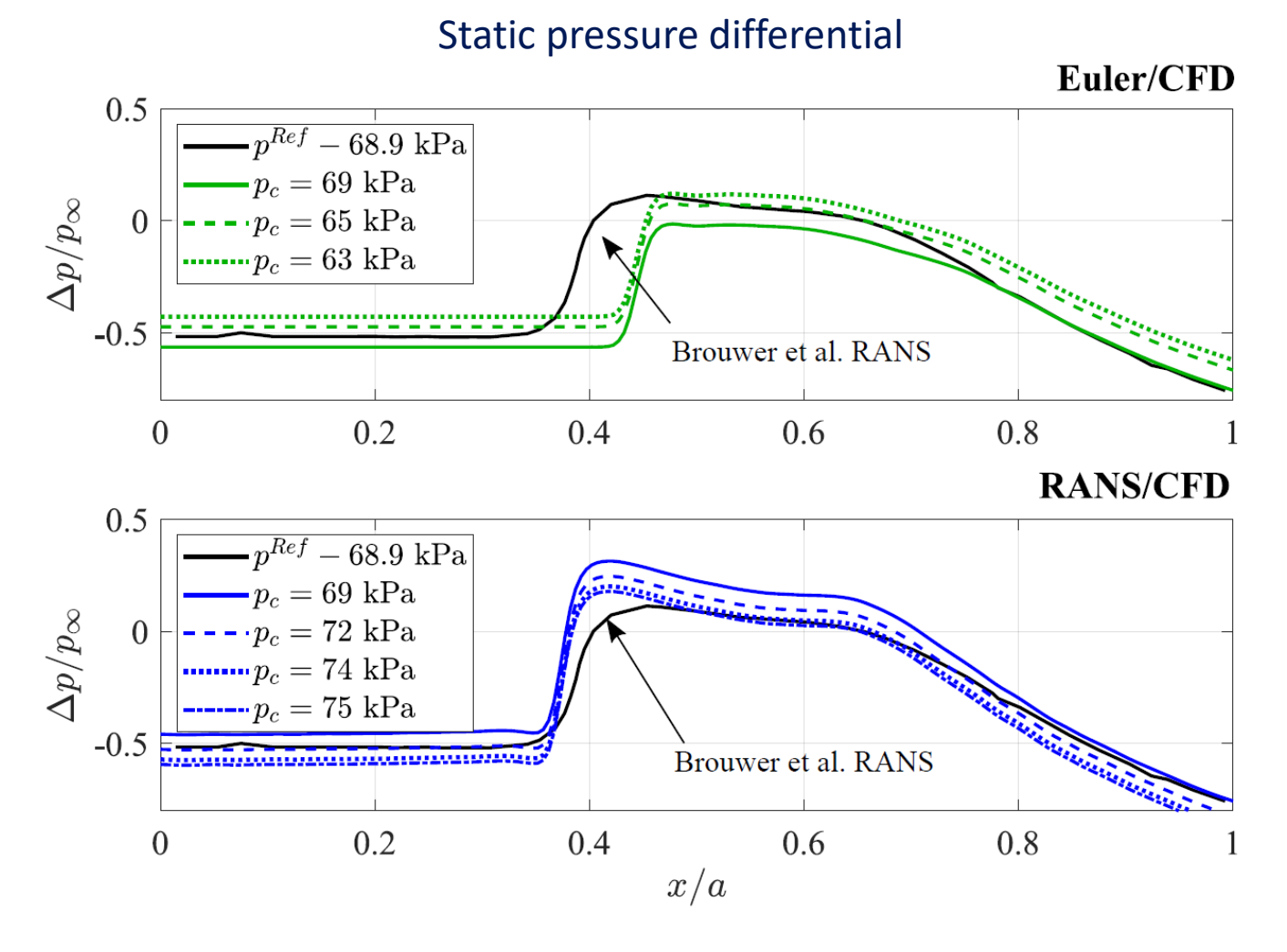


Static pressure



Shock Impingement Aerodynamic Properties

Steady Solution



Panel stiffened by the Δp effect

Conclusion

- A range of aerodynamic models has been considered including Linear Piston Theory and Full Potential Flow for the no-shock case, and Euler and RANS/DLTA for the shock impingement case.
- For the RC-19 configuration the results are particularly sensitive to the pressure differential, thermal stress (which leads to buckling) and the in-plane as well as out of plane boundary support conditions for the plate.
- Results for flutter and LCO of the RC-19 experiment are not particularly sensitive to the aerodynamic model, with the key exception that when using the DLTA/CFD method, the steady solution for the shock location/magnitude can present indirect implications in the LCO prediction.

The computational models agree with the observations from experiments **on the essentials of the physical phenomena** e.g. buckling, flutter and limit cycle oscillations.

There is broad quantitative agreement between computations and experiments, given the sensitivity of the results to a wide range of parameters.



Correlation of Mathematical Model with AFRL RC-19 Aerothermoelastic Experiment Including an Impinging Shock

AIAA AVIATION Forum 2025

Luisa Piccolo Serafim and Earl Dowell – Duke University

Kirk Brouwer – AFRL, Wright-Patterson AFB

July 22, 2025 | Las Vegas, NV

